

# On the Einstein-Cartan cosmology vs. Planck data

Davor Palle

*Zavod za teorijsku fiziku, Institut Rugjer Bošković*

*Bijenička cesta 54, 10000 Zagreb, Croatia*

(Dated: September 20, 2013)

## Abstract

The first comprehensive analyses of Planck data reveal that the cosmological model with dark energy and cold dark matter can satisfactorily explain the essential physical features of the expanding Universe. However, the inability to simultaneously fit large and small scale TT power spectrum, scalar power index smaller than one and the observations of the violation of the isotropy found by few statistical indicators of the CMB, urge theorists to search for explanations. We show that the model of the Einstein-Cartan cosmology with clustered dark matter halos and their corresponding clustered angular momenta coupled to torsion, can account for small scale - large scale discrepancy and larger peculiar velocities (bulk flows) for galaxy clusters. The nonvanishing total angular momentum (torsion) of the Universe enters as a negative effective density term in the Einstein-Cartan equations causing partial cancellation of the mass density. The integrated Sachs-Wolfe contribution of the Einstein-Cartan model is negative, thus it can provide partial cancellation of the large scale power of the TT CMB spectrum. The observed violation of the isotropy appears as a natural ingredient of the Einstein-Cartan model caused by the spin densities of light Majorana neutrinos in the early stage of the evolution of the Universe and bound to the lepton CP violation and matter-antimatter asymmetry.

PACS numbers: 98.80.Es; 12.10.Dm; 04.60.-m

## I. INTRODUCTION AND MOTIVATION

Although the presence of dark matter and dark energy is justified by all cosmological observations, their identification and properties are still far from being established. The measurements of the fluctuations of the CMB are in this respect especially valuable because of the wealth and accurate information that can be extracted from them.

The most recent disclosed results of the Planck mission contain issues like: the temperature power spectrum, gravitational lensing or integrated Sachs-Wolfe effect, up to Sunyaev-Zeldovich cluster counts, isotropy, nonGaussianity or cosmic infrared background. It seems that the old, unexpected features, beyond the  $\Lambda$ CDM + inflation model, persist in data and are even more highlighted: 1. large scale temperature power spectrum much lower than the  $\Lambda$ CDM prediction, not limited only to low quadrupole [1] but to almost all multipole moments  $l < 30$  (see Fig. 37 in ref. [2]), 2. scalar power spectrum index less than 1 (see Table 8 in ref. [2]), 3. violation of isotropy observed as hemispherical asymmetry, parity asymmetry, quadrupole-octopole alignment, cold spot, and dipolar asymmetry [3].

If the violation of isotropy will be confirmed by other complementary cosmic observations of radio galaxies [4], spiral galaxies [5], bulk flows of clusters [6] or quasars [7], it will challenge cosmological principles and call for the new theoretical insights.

Assuming that the observed anomalies are real phenomena, we try to understand and elucidate measured physical features by the Einstein-Cartan (EC) cosmology. Incorporating rotating degrees of freedom of matter (spin and angular momentum) and spacetime (torsion) into the relativistic framework, the EC cosmology appears as a nonsingular theory [8, 9], the cosmic mass density can be fixed [9], the scalar power index can acquire the negative tilt [10], spin densities trigger density fluctuations [11] and the right-handed vorticity (rotation) of the Universe [12] resulting at later stages of the evolution in the nonvanishing total angular momentum of the Universe [13]. The nonsingular EC cosmology is in conformity with the nonsingular theory of gauge interactions in particle physics [14] that contains light and heavy Majorana neutrinos as hot and cold dark matter particles [15], including other important implications of the perturbative and nonperturbative aspects of strong and electroweak interactions phenomenology [16].

In this paper we investigate and compare EC and  $\Lambda$ CDM cosmologies solving evolution equations for the scale dependent density contrasts, mass fluctuations, peculiar velocities,

and integrated Sachs-Wolfe effect. The next chapter contains description of the evolution equations, definitions and the introduction of our simple clustering model. The concluding section deals with the numerical results of the computations, comparisons of the EC, and  $\Lambda$ CDM cosmologies and final remarks and hints for future research.

## II. DEFINITIONS, EQUATIONS AND CLUSTERING MODEL

Because any deviation from cosmic homogeneity and isotropy is very small, we limit our considerations to the homogeneous and isotropic geometry. We start the evolution in the radiation era when clustering of dark and baryonic matter is negligible. The evolution equations for matter density contrasts in Fourier space are derived in [17]

$$\begin{aligned}\frac{d^2 h}{dt^2} + \frac{2}{a} \frac{da}{dt} \frac{dh}{dt} &= 8\pi G_N (2\rho_r \delta_r + \rho_m \delta_m), \\ \frac{d\delta_m}{dt} &= \frac{1}{2} \frac{dh}{dt}, \quad \frac{d\delta_r}{dt} = \frac{4}{3} \left( \frac{kv}{a} + \frac{1}{2} \frac{dh}{dt} \right), \\ \frac{dv}{dt} &= -k \frac{\delta_r}{4a}, \quad \left( \frac{da}{dt} \right)^2 = \frac{8}{3} \pi G_N a^2 (\rho_r + \rho_m + \rho_\Lambda).\end{aligned}\tag{1}$$

We here use the notation  $h = \sum_{\alpha=1}^3 h_\alpha^\alpha$ ,  $g_{\alpha\beta} = -a^2[\delta_{\alpha\beta} - h_{\alpha\beta}]$ , density contrasts are  $\delta_i = \frac{\delta\rho_i}{\rho_i}$ ,  $k$  is the comoving wave number,  $a = \frac{R}{R_0} = \frac{1}{1+z}$ , subscripts m,r, $\Lambda$  denote matter, radiation and the cosmological constant quantities, respectively, and  $v$  is a velocity. All the quantities are functions of  $t$  and  $\vec{k}$ .

These equations can be cast into the more suitable form by getting rid of  $h = \sum_{\alpha=1}^3 h_\alpha^\alpha$  and by changing the evolution variable to  $y = \ln a$ :

$$\begin{aligned}\frac{d^2 \delta_m}{dy^2} &= -\frac{1}{2} \frac{d\delta_m}{dy} \Omega_m (\Omega_r a^{-1} + \Omega_m + \Omega_\Lambda a^3)^{-1} + \frac{3}{2} (2\Omega_r \delta_r + \Omega_m a \delta_m) (\Omega_r + \Omega_m a + \Omega_\Lambda a^4)^{-1}, \\ \frac{d\delta_r}{dy} &= \frac{4}{3} \left( \frac{d\delta_m}{dy} + \frac{kv}{\dot{a}} \right), \quad \frac{dv}{dy} = -\frac{\delta_r}{4} \frac{k}{\dot{a}}.\end{aligned}\tag{2}$$

Our notation includes  $\rho_r = \Omega_r \rho_c a^{-4}$ ,  $\rho_m = \Omega_m \rho_c a^{-3}$ ,  $\rho_\Lambda = \Omega_\Lambda \rho_c$ ,  $\rho_c = \frac{3H_0^2}{8\pi G_N}$ ,  $H_0 = 100h \text{ km s}^{-1} \text{ Mpc}^{-1}$  and  $\dot{a} = 3.2409 \times 10^{-18} h [\Omega_r a^{-2} + \Omega_m a^{-1} + \Omega_\Lambda a^2]^{1/2} s^{-1}$ .

The evolution equations for the EC cosmology (neglecting small vorticity and acceleration  $\omega = m = 0$ ,  $\lambda = 0$ ;  $Q = Q_0 a^{-3/2} = \textit{torsion}$ ) are derived in [13] (eq. (14)):

$$\begin{aligned}
\ddot{\delta}_1 + 2\frac{\dot{a}}{a}\dot{\delta}_1 - 2Q\dot{\delta}_2 + \left(-\frac{1}{3}\kappa\Lambda - \frac{5}{3}Q^2 - \frac{1}{3}\kappa\rho + \frac{\ddot{a}}{a}\right)\delta_1 + \frac{1}{4}\frac{\dot{a}}{a}Q\delta_2 &= 0, \\
\ddot{\delta}_2 + 2\frac{\dot{a}}{a}\dot{\delta}_2 + 2Q\dot{\delta}_1 + \left(-\frac{1}{3}\kappa\Lambda - \frac{5}{3}Q^2 - \frac{1}{3}\kappa\rho + \frac{\ddot{a}}{a}\right)\delta_2 - \frac{1}{4}\frac{\dot{a}}{a}Q\delta_1 &= 0, \\
\ddot{\delta}_3 + 2\frac{\dot{a}}{a}\dot{\delta}_3 + \left(-\frac{1}{3}\kappa\Lambda - \frac{2}{3}Q^2 - \frac{1}{3}\kappa\rho + \frac{\ddot{a}}{a}\right)\delta_3 &= 0, \\
\delta &\equiv [\delta_1^2 + \delta_2^2 + \delta_3^2]^{1/2}.
\end{aligned} \tag{3}$$

We assume that after redshift  $z_G = 10$  the nonlinear bound structures are formed in the form of stars, galaxies, and clusters. The clustering of particles forming halos are described by a model with only two parameters  $k_G$  and  $\sigma_G$ . This is applied to both mass and angular momentum clustering:

$$\begin{aligned}
Q(a) &= (2\pi)^{-3} \int d^3k \hat{Q}(a, \vec{k}) = Q_0 a^{-3/2} \Theta(z_G - z), \\
\hat{Q}(a, \vec{k}) &= \bar{Q}_0 a^{-3/2} e^{-|k-k_G|/\sigma_G} \Theta(z_G - z) \Rightarrow Q_0 = \bar{Q}_0 (2\pi)^{-3} \int d^3k e^{-|k-k_G|/\sigma_G},
\end{aligned} \tag{4}$$

$$\begin{aligned}
\rho(a) &= (2\pi)^{-3} \int d^3k \hat{\rho}(a, \vec{k}) = \rho_0 a^{-3} \Theta(z_G - z), \\
\hat{\rho}(a, \vec{k}) &= \bar{\rho}_0 a^{-3} e^{-|k-k_G|/\sigma_G} \Theta(z_G - z) \Rightarrow \rho_0 = \bar{\rho}_0 (2\pi)^{-3} \int d^3k e^{-|k-k_G|/\sigma_G},
\end{aligned} \tag{5}$$

Fourier transforms of the evolution equations (3) take now the following form with the evolution variable  $y = \ln a$ :

$$\begin{aligned}
\left(\frac{\dot{a}}{a}\right)^2 \frac{d^2 \Delta_{1,2}}{dy^2} + \frac{\dot{a}}{a} \left(\frac{d\dot{a}}{da} + \frac{\dot{a}}{a}\right) \frac{d\Delta_{1,2}}{dy} \mp 2\frac{\dot{a}}{a} \langle Q \frac{d\delta_{2,1}}{dy} \rangle_{FT} + \left(-\frac{1}{3}\kappa\Lambda + \frac{\ddot{a}}{a}\right) \Delta_{1,2} \\
- \frac{1}{3}\kappa \langle \rho_m \delta_{1,2} \rangle_{FT} - \frac{5}{3} \langle Q^2 \delta_{1,2} \rangle_{FT} \pm \frac{1}{4} \frac{\dot{a}}{a} \langle Q \delta_{2,1} \rangle_{FT} = 0, \\
\left(\frac{\dot{a}}{a}\right)^2 \frac{d^2 \Delta_3}{dy^2} + \frac{\dot{a}}{a} \left(\frac{d\dot{a}}{da} + \frac{\dot{a}}{a}\right) \frac{d\Delta_3}{dy} + \left(-\frac{1}{3}\kappa\Lambda + \frac{\ddot{a}}{a}\right) \Delta_3 - \frac{1}{3}\kappa \langle \rho_m \delta_3 \rangle_{FT} - \frac{2}{3} \langle Q^2 \delta_3 \rangle_{FT} = 0.
\end{aligned} \tag{6}$$

The Einstein-Cartan field equations define the cosmic clocks (see eq. (15) of [13]) as follows:

$$\begin{aligned}
\dot{a} &= H_0 [\Omega_m a^{-1} + \Omega_\Lambda a^2 - \frac{1}{3} a^2 Q^2]^{1/2}, \\
\frac{d\dot{a}}{da} &= H_0 \frac{1}{2} [\Omega_m a^{-1} + \Omega_\Lambda a^2 - \frac{1}{3} a^2 Q^2]^{-1/2} [-\Omega_m a^{-2} + 2\Omega_\Lambda a + \frac{1}{3} a Q^2], \\
\frac{\ddot{a}}{a} &= \frac{1}{3}\kappa\Lambda - \frac{1}{6}\kappa\rho + \frac{2}{3}Q^2.
\end{aligned} \tag{7}$$

The following definitions and convolutions are used in eq. (6):

$$\begin{aligned}
\Delta_i(y, \vec{k}) &\equiv \int d^3x e^{i\vec{k}\cdot\vec{x}} \delta_i(y, \vec{x}), \\
\langle Q\delta_i \rangle_{FT}(y, \vec{k}) &\equiv \int d^3x e^{i\vec{k}\cdot\vec{x}} Q(y, \vec{x}) \delta_i(y, \vec{x}) = (2\pi)^{-3} \int d^3k' Q(y, \vec{k} - \vec{k}') \Delta_i(y, \vec{k}'), \\
\langle Q^2\delta_i \rangle_{FT}(y, \vec{k}) &\equiv \int d^3x e^{i\vec{k}\cdot\vec{x}} Q^2(y, \vec{x}) \delta_i(y, \vec{x}) \\
&= (2\pi)^{-6} \int d^3k' d^3k'' \Delta_i(y, \vec{k}') Q(y, \vec{k}'') Q(y, \vec{k} - \vec{k}' - \vec{k}'').
\end{aligned}$$

Having all the evolution equations for the EC and  $\Lambda$ CDM cosmologies, we define initial conditions in the radiation era and choose the parameters of the models:

$$\begin{aligned}
a_i &= 10^{-8}, \quad \delta_r(a_i) = k^{1/2} a_i^2, \quad \delta_m(a_i) = \frac{3}{4} k^{1/2} a_i^2, \quad y = \ln a, \\
\frac{d\delta_r}{dy}(a_i) &= 2k^{1/2} a_i^2, \quad \frac{d\delta_m}{dy}(a_i) = \frac{3}{2} k^{1/2} a_i^2, \quad v(a_i) = 0, \\
\Lambda\text{CDM} : \Omega_m &= 0.34, \quad \Omega_\Lambda = 0.66, \quad Q = 0, \quad h = 0.67, \\
EC : \Omega_m &= 2, \quad \Omega_\Lambda = 0, \quad h = 0.67, \quad Q = \begin{cases} 0 & \text{if } z > 10 \\ -2.3a^{-3/2} & \text{if } 1 < z \leq 10 \\ -\sqrt{3}a^{-3/2} & \text{if } 0 \leq z \leq 1 \end{cases}
\end{aligned}$$

Our choice of the torsion (angular momentum) parameters is guided by the condition that at zero redshift  $\Omega_Q \simeq -1$  [9, 13] (at the redshifts  $1 \geq z \geq 0$  the galaxy clusters emerge changing the total angular momentum contribution of the era  $z > 1$ ), while at the earlier epoch  $10 > z > 1$  our choice is guided by the condition to match roughly the correct cosmic clocks and the age of the Universe:

$$\begin{aligned}
\tau_U(\text{Gyr}) &= \frac{10}{h} \int_{10^{-3}}^1 \frac{da}{a} [\Omega_\Lambda + \Omega_m a^{-3} - \frac{1}{3} Q^2]^{-1/2}, \\
\tau_U(\Lambda\text{CDM}) &= 13.89 \text{Gyr}, \quad \tau_U(\text{EC}) = 13.29 \text{Gyr}, \\
k_{min} &= 10^{-3} \text{Mpc}^{-1}, \quad k_{max} = 10^2 \text{Mpc}^{-1}, \quad k_G = 1 \text{Mpc}^{-1}, \quad \sigma_G = 0.25 \text{Mpc}^{-1}.
\end{aligned}$$

We integrate the above evolution equations to the relative accuracy  $\mathcal{O}(10^{-4})$  by lowering the integration steps until the required accuracy is reached. Equations (2) are solved for the evolution from  $a_i = 10^{-8}$  up to  $a_G = 1/(1 + z_G)$  and Eqs. (6) are then solved from  $a_G = 1/(1 + z_G)$  up to  $a = 1$ . The Adams-Bashforth-Moulton predictor-corrector method

is used for differential equation integrations (code of L. F. Shampine and M. K. Gordon, Sandia Laboratories, Albuquerque, New Mexico) and CUBA library for multidimensional integrations [18]. The next section is devoted to the detailed exposure of the numerical results and comparison between EC and  $\Lambda$ CDM models. The relevance of the results for the Planck data are given here as well.

### III. RESULTS, DISCUSSION AND CONCLUSIONS

Because the best fit to the Planck temperature power spectrum is dominantly performed by the multipoles  $l > 30$ , it is not a surprise that the concordance  $\Lambda$ CDM model is favoured, but at the expense of the wrong fit for low multipoles (large scales). By solving evolution equations for the EC and  $\Lambda$ CDM with the simple clustering model, one can verify that at low redshifts these two models produce density contrasts that differ substantially at large scales, while being similar at smaller scales (see Fig. 1).

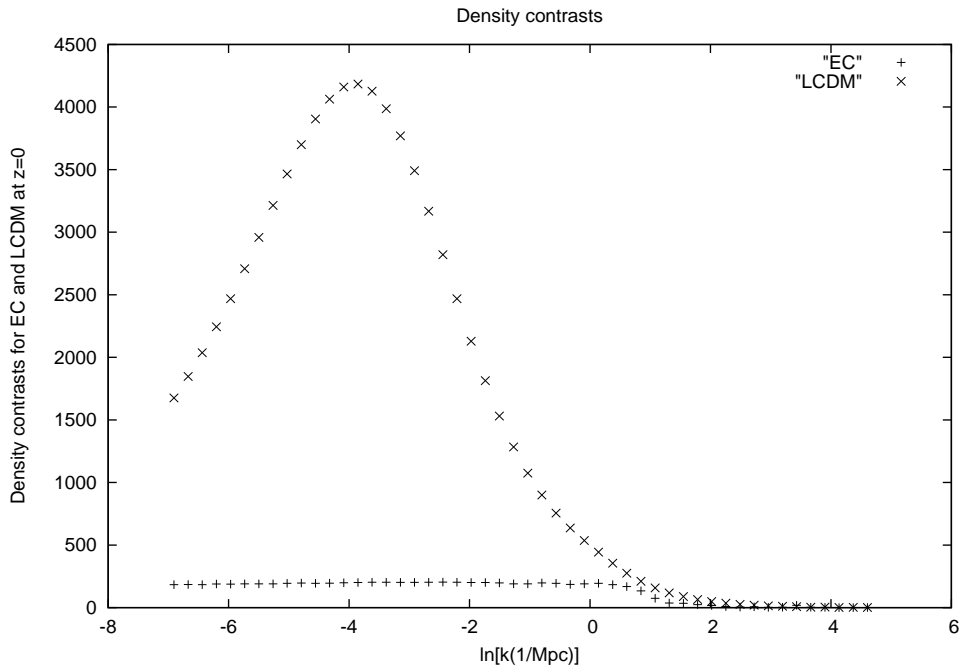


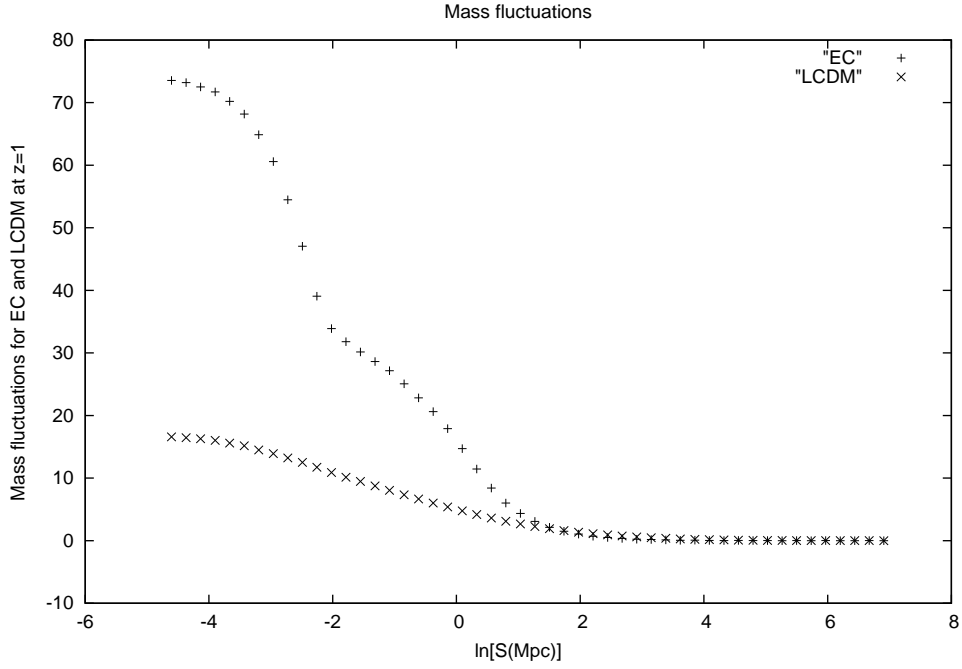
**Fig. 1: Density contrasts at  $z=0$  as functions of the wave number  $k(Mpc^{-1})$  normalized at  $k_{max} : \delta_m(k_{max}) = 1$ .**

If we accept the following normalization on a larger scale [13]:

$$(\delta M/M)_{RMS}(a = 1, S_0 = 10h^{-1}Mpc) = 1.$$

the processed spectrum of the mass fluctuations with the top hat window function for EC and  $\Lambda$ CDM models then differ at small scales (see Fig. 2):

$$\begin{aligned} (\delta M/M)_{RMS}^2(a, S) &\equiv N^{-1} \int d^3k W^2(\vec{k}, S) |\delta(a, \vec{k})|^2, \\ N &= \int d^3k W^2(\vec{k}, S_0) |\delta(a = 1, \vec{k})|^2, \\ W(y = kS) &= \frac{3}{y^3} (\sin y - y \cos y). \end{aligned} \quad (8)$$



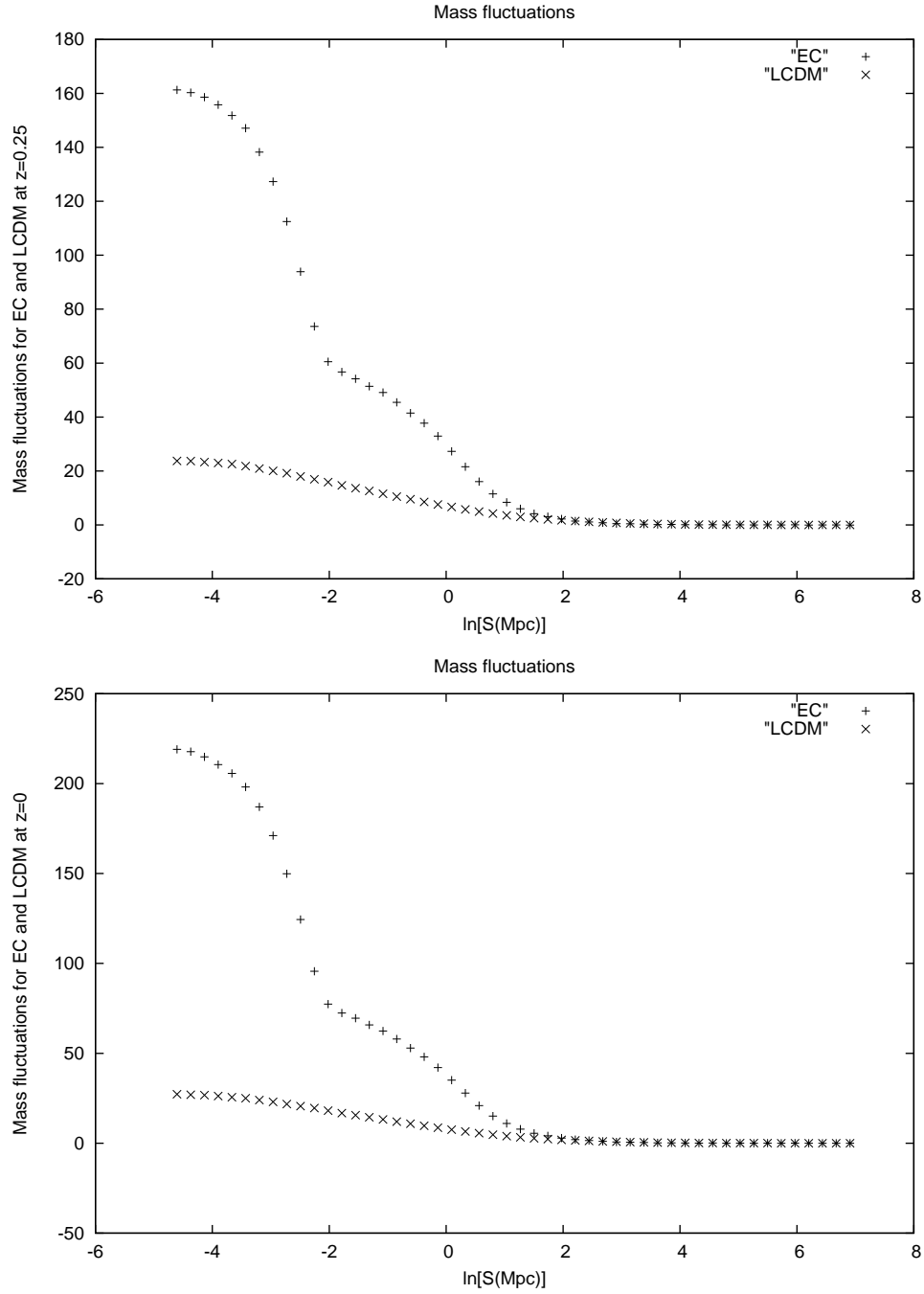
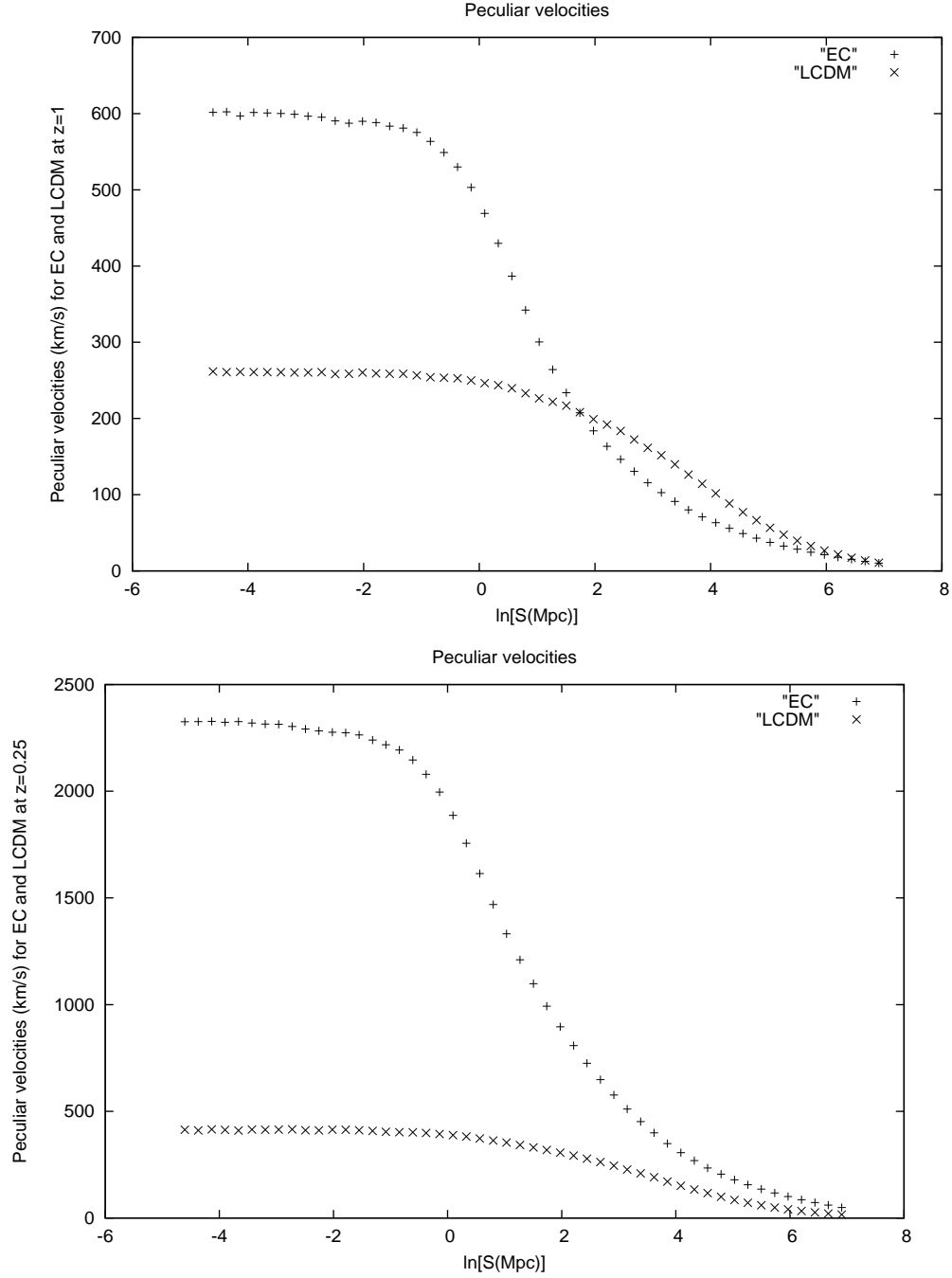


**Fig. 2:** Mass fluctuations for three redshifts ( $z=0;0.25;1$ ) as functions of the scale  $S(\text{Mpc})$ .

We can similarly evaluate the peculiar velocities as functions of the scale and redshift with the same normalization as in eq.(8):

$$v_{RMS}^2(a, S) \equiv N^{-1} \int d^3k W^2(\vec{k}, S) \frac{1}{\vec{k}^2} \left| a \dot{a} \frac{d\delta(a, \vec{k})}{da} \right|^2, \quad (9)$$

giving the expected results (see Fig. 3), where the EC cosmology produces larger peculiar velocities than the  $\Lambda$ CDM cosmology at the galaxy and galaxy cluster scales  $\mathcal{O}(10^{-1})Mpc - \mathcal{O}(10^2)Mpc$ .



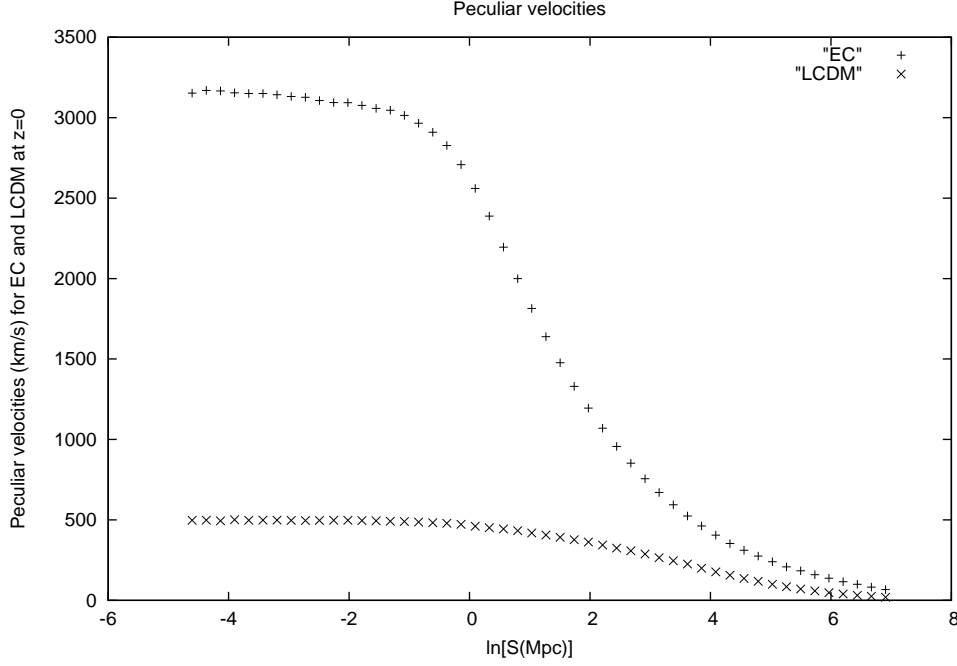


**Fig. 3: Peculiar velocities for three redshifts ( $z=0;0.25;1$ ) as functions of the scale  $S(\text{Mpc})$ .**

The conclusions are not sensitive to the reasonable choices of the parameters of the clustering model. The integrated Sachs-Wolfe (ISW) effect plays an important role at low redshifts in the evolution, if the mass density differs from one [13]:

$$a_{lm}^{ISW} = 12\pi^l \int d^3k Y_l^{m*}(\hat{k}) \delta_{\bar{k}} \left(\frac{H_0}{k}\right)^2 \int da j_l(kr) \chi^{ISW}, \quad (10)$$

$$\chi^{ISW}(a) = -\Omega_m \frac{d}{da} (\delta(a)/a), \quad r = \int_a^1 da a^{-2} H^{-1}(a), \quad \delta(a=1) = 1.$$

The ISW is positive (negative) for the  $\Lambda\text{CDM}$  (EC) cosmology (see Fig. 4). The structure of the EC ISW curve around  $z=1$  is just an artefact of our simple model for torsion with a nonanalytic behaviour at  $z=1$ .

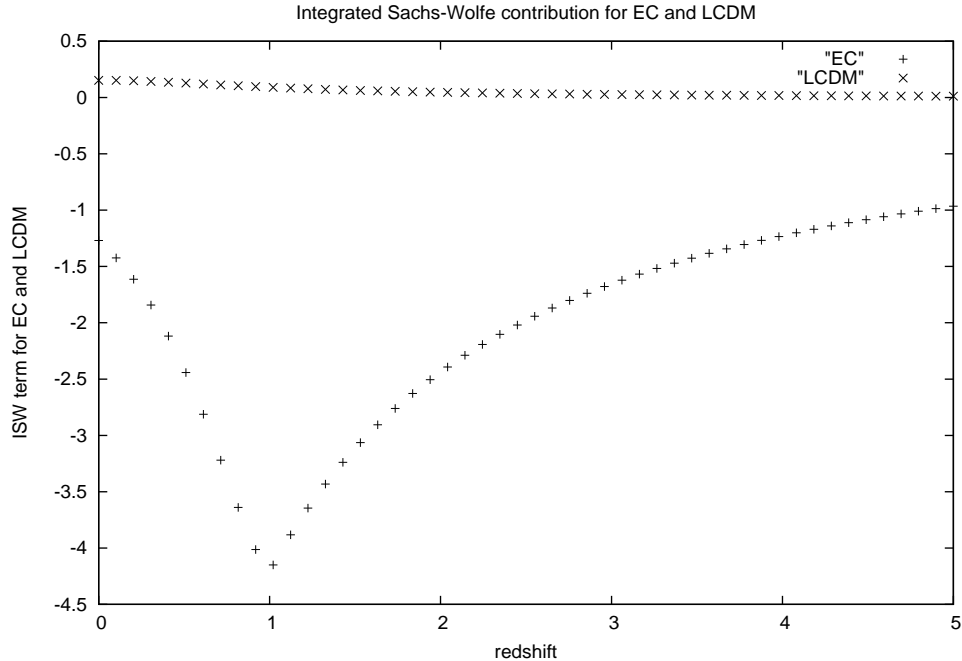


**Fig. 4: Integrated Sachs-Wolfe terms  $\chi^{ISW}$  for EC and  $\Lambda$ CDM cosmologies.**

The compendium of all our results can be summarized as follows: (1) the  $\Lambda$ CDM model cannot simultaneously fit the large and the small scale parts of the Planck TT spectrum, while the EC can rectify this deficiency owing to the presence of the new rotational degrees of freedom (torsion) that partially cancels the large mass density ( $\Omega_m = 2$ ) when clustering matters, i.e. the rotation (centripetal force) acts opposite to the attractive force of gravity, (2) the presence of the ISW effect is observed in Planck data [19], but with the unknown sign; the very small low multipoles of the Planck TT spectrum imply the negative contribution of the ISW [20], thus in accord with the EC model, (3) the peculiar velocities are larger at the galaxy and galaxy cluster scales for the EC than  $\Lambda$ CDM cosmologies at low redshifts. These conclusions are robust and are qualitatively valid for the reasonable variation of the clustering model parameters  $k_G$  and  $\sigma_G$ . The two different analyses of the Planck peculiar velocities of galaxy clusters [21] are still not conclusive as to whether the data are consistent with the  $\Lambda$ CDM model or not.

Our final remark is that the first Planck results favour a description of the Universe with the anisotropic models. The  $\Lambda$ CDM and the inflationary paradigm cannot fulfil severe phenomenological requirements. We show that the EC cosmology with the new rotational degrees of freedom can resolve almost all of the  $\Lambda$ CDM model deficiencies. However, the

N-body numerical simulations, including the angular momenta of the CDM halos and their feedback onto the background cosmic geometry, have to be applied within the EC gravity.

---

- [1] C. L. Bennett et al., *Astrophys. J. Suppl. Ser.* **148**, 1 (2003).
- [2] Planck Collab., arXiv:1303.5075.
- [3] Planck Collab., arXiv:1303.5083.
- [4] P. Birch, *Nature*, **298**, 451 (1982).
- [5] M. J. Longo, *Phys. Lett. B* **699**, 224 (2011).
- [6] A. Kashlinsky, F. Atrio-Barandela, D. Kocevski and H. Ebeling, *Astrophys. J. Lett.* **686**, L49 (2008).
- [7] D. Hutsemékers, *Astron. and Astrophys.* **332**, 410 (1998).
- [8] A. Trautman, *Nature* **242**, 7 (1973).
- [9] D. Palle, *Nuovo Cim. B* **111**, 671 (1996).
- [10] D. Palle, *Nuovo Cim. B* **122**, 67 (2007).
- [11] D. Palle, *Nuovo Cim. B* **114**, 853 (1999).
- [12] D. Palle, *Entropy* **14**, 958 (2012).
- [13] D. Palle, *Eur. Phys. J. C* **69**, 581 (2010).
- [14] D. Palle, *Nuovo Cim. A* **109**, 1535 (1996).
- [15] D. Palle, *Nuovo Cim. B* **115**, 445 (2000); *ibidem* **118**, 747 (2003).
- [16] D. Palle, *Hadronic J.* **24**, 87 (2001); *ibidem* **24**, 469 (2001); D. Palle, *Acta Phys. Pol. B* **43**, 1723 (2012); *ibidem* **43**, 2055 (2012); D. Palle, arXiv:1210.4404.
- [17] P. J. E. Peebles, *The Large-Scale Structure of the Universe* (Princeton University Press, New Jersey, 1980); P. J. E. Peebles, *Astrophys. J.* **277**, 470 (1984).
- [18] T. Hahn, *Comp. Phys. Commun.* **168**, 78 (2005).
- [19] Planck Collab., arXiv:1303.5079.
- [20] H. Kodama and M. Sasaki, *Prog. Theor. Phys. Suppl.* **78**, 1 (1984).
- [21] Planck Collab., arXiv:1303.5090; F. Atrio-Barandela, arXiv:1303.6614 (to appear in *Astron. and Astrophys.*).